

## Plasma dynamics in the night-time *F*-region at Arecibo

R. G. BURNSIDE, J. C. G. WALKER

Space Physics Research Laboratory, Department of Atmospheric and Oceanic Science, University of Michigan, Ann Arbor, MI 48109, U.S.A.

R. A. BEHNKE and C. A. TEPLEY

Arecibo Observatory, P.O. Box 995, Arecibo, Puerto Rico 00613, U.S.A.

(Received for publication 5 March 1985)

**Abstract**—Incoherent scatter radar observations of the night-time *F*-layer at Arecibo, Puerto Rico, are used to determine horizontal gradients in peak electron density and the *F*-layer height. At certain times of night, in both the summer and winter, the horizontal gradients in these parameters may be significant. The continuity equation for  $O^+$  is used to examine the sources and sinks of plasma at the peak of the night-time *F*-layer. In summer, before midnight, the *F*-layer is sufficiently elevated that chemical recombination at the peak is very slow. At these times we find that the local peak electron density may be significantly influenced by horizontal (predominantly eastward) advection or convergence of plasma. In winter, horizontal advection is usually less important than plasma convergence and chemical loss.

### 1. INTRODUCTION

For many years now, information on *F*-region plasma dynamics has been obtained with the incoherent scatter radar at the Arecibo Observatory in Puerto Rico. A wide variety of ionospheric phenomena have been studied, for example: night-time polarization electric fields (BEHNKE and HAGFORS, 1974; BURNSIDE *et al.*, 1983a); disturbed electric fields (GONZALES *et al.*, 1983); mid-latitude spread-*F* (IMEL *et al.*, 1981). Plasma velocity measurements have also been used to infer the meridional component of the thermospheric neutral velocity (HARPER, 1973; BURNSIDE *et al.*, 1983b).

Spatial variations in layer height in the nocturnal *F*-region at Arecibo were first reported by BEHNKE (1979). With this exception, however, work with Arecibo data has been mainly limited to examining temporal or altitudinal variations of electron density, ion velocity and temperature (see, for example, FUKAO *et al.*, 1979; EMERY *et al.*, 1981). Presumably, the reason for this emphasis is that the Arecibo radar is restricted to a maximum effective zenith angle of 15°. In contrast with Arecibo, the fully-steerable radars at Millstone Hill and Chatanika (now at Søndre Strømfjord) have been used very effectively to obtain spatial maps of a wide range of ionospheric parameters (see, for example, EVANS *et al.*, 1983; VONDRAK and RICH, 1982; KELLY, 1983). In this paper we will show that spatial variations in electron density, *F*-layer height and, indirectly, certain com-

ponents of ion velocity may also be determined with reasonable precision from incoherent scatter measurements at Arecibo.

Arecibo is located at a dip latitude of 31°N, which is some 1500 km north of the peak of the Appleton anomaly. As well as the work of BEHNKE (1979), a considerable amount of indirect evidence obtained at Arecibo suggests that horizontal gradients in electron density and ion velocity are significant on spatial scales of the order of 1000 km. BURNSIDE *et al.* (1981) observed latitudinal convergence in the meridional component of the neutral wind near midnight at Arecibo. Large gradients in 630.0 nm nightglow intensity, reported by HERRERO and MERIWETHER (1980), were identified with latitudinal gradients in the height of the *F*-layer. Theoretical calculations (see, for example, ANDERSON, 1981) also lead us to expect that significant latitudinal gradients in peak electron density may exist at certain times of the night at Arecibo.

The experimental method is described in Section 2 of this paper. In Section 3 we discuss the determination of the horizontal gradients in peak electron density and *F*-layer height. Data from different seasons have been analysed and significant spatial gradients have been found, both in summer and winter.

In Section 4 we try to assess whether horizontal advection of plasma plays a significant role in the dynamics of the night-time *F*-layer at Arecibo. This

is done by evaluating the magnitude of the various terms in the  $O^+$  continuity equation. Some simplification (without loss of any essential physics) is achieved by restricting the calculation to the  $F$ -layer peak. Below the peak, chemical loss and vertical transport dominate the continuity equation. However, at higher altitudes, recombination is slow and horizontal advection and ion velocity divergence may become significant. Although this study is restricted to the altitude of the  $F$ -layer peak, the layer height often changes markedly during the course of a night at Arecibo, with associated changes in the importance of transport and recombination.

In previous studies using the continuity equation, such as those by JAIN and WILLIAMS (1974), EVANS (1975) and FUKAO *et al.* (1979), it was assumed that the ionosphere is horizontally stratified. We examine this assumption, and find that it is not particularly good when the  $F$ -layer is high. Although we are able to evaluate the horizontal advection terms in the continuity equation, some approximations are still necessary, because there is no direct way of measuring the horizontal gradients in the various components of the ion velocity vector. Nevertheless, some of these gradients may be inferred. For example, by evaluating an integrated form of the ion continuity equation, we are able to estimate the horizontal gradient in the vertical ion velocity.

Section 5 is a summary and discussion of the results of this work.

## 2. EXPERIMENTAL

Incoherent scatter measurements of electron density and ion velocity are obtained using the beam-swinging technique described by HAGFORS and BEHNKE (1974) and BEHNKE (1979). Two different pulse schemes are interwoven. For 75% of the observing time, single 300  $\mu$ s pulses are transmitted. The autocorrelation function of the received signal is analysed to give the line-of-sight ion velocity and the ion and electron temperatures. For the remainder of the observing time, a 13 baud Barker coded signal is transmitted in order to obtain an electron density profile with a height resolution of 600 m. These measurements are then averaged to give electron densities at 4.8 km intervals from 80 to 540 km. Drifts in the sensitivity of the radar are accounted for by regular calibrations against a stable noise source. Ionosonde measurements of  $foF2$  are used to provide an absolute calibration. This is a standard  $F$ -region program that is used to make observations at Arecibo on Regular World Days.

Line-of-sight ion velocities are obtained at 12 azimuths and at 5 altitudes from 250 to 480 km. The horizontal components of the ion velocity vector are determined at each height by Fourier analysis of the variation in the line-of-sight velocity with azimuth (HAGFORS and BEHNKE, 1974). This analysis requires the assumption that the velocity at each height does not change significantly during the 16 min required to complete a 360° swing of the radar beam. In practice, we average the velocities determined from consecutive clockwise and anticlockwise swings of the radar beam. This procedure will account for any changes in ion velocity that are linear in time.

For this study it is necessary to determine the height derivative of certain components of the ion velocity. This is done by fitting a straight line to the measurements at the 5 different heights. With the possible exception of the vertical component, the precision of the measurements is insufficient to justify the use of higher order terms. When the layer peak is below 350 km, measurements from all 5 heights are used to determine the altitudinal variation of each velocity component. At times when the layer peak is above 350 km, the electron density at 250 km is usually very low, and the velocity measurement at this height is too noisy to be meaningful. In these cases the gradient is determined from the measurements at the 4 heights above 300 km.

## 3. HORIZONTAL GRADIENTS IN ELECTRON DENSITY AND LAYER HEIGHT

### 3.1. Data analysis

The Barker code data are averaged over 8 adjacent altitudes to obtain a set of 70 electron density measurements between 180 and 520 km. After discarding any densities less than  $3 \times 10^4 \text{ cm}^{-3}$  (i.e. at low altitudes), a Chapman profile is fitted to the data. The form of the Chapman function has 6 free parameters and is discussed in more detail by BURNSIDE *et al.* (1983b). This procedure, which greatly reduces the scatter in the data, is carried out for each of the 12 azimuths that comprise a complete 360° swing of the radar beam. Next, the azimuthal variation of electron density is analysed at each height by fitting a sine function to the smoothed data points. The spatial gradients that we derive in this way are the derivatives in a set of first order, two dimensional Taylor expansions of the electron density about a set of locations spaced 4.8 km vertically apart directly above Arecibo.

The peak electron density,  $N_m$ , and the height of the peak,  $h_m$ , are obtained at each azimuth directly from the Chapman fit. The same Fourier analysis is then used to calculate the spatial gradients in  $N_m$  and  $h_m$ . If a significant temporal change occurs during the 16 min required for a full swing of the radar beam, it will lead to an error in the derived spatial gradient. We account for this effect by averaging the two spatial gradients determined from consecutive clockwise and anticlockwise swings. Because  $N_m$  tends to change more slowly than  $h_m$ , the derived horizontal gradients in  $N_m$  are less affected by temporal changes. Similarly, the time derivative of  $N_m$  (see Section 4) is calculated using measurements spaced 16 min apart, and then two consecutive determinations of  $\partial N_m / \partial t$  are averaged. In this paper we use a geomagnetic coordinate system, where  $x$  is positive southward,  $y$  is positive eastward and  $z$  is positive upward.

3.2. Results

As an example, the derived values of peak electron density,  $N_m$ , and layer height,  $h_m$ , for the night of 17–18 August 1982 are shown in Fig. 1. The azimuthal variation in  $N_m$  is particularly strong from 2200 to 0200 AST, with enhanced electron density toward the southeast (Fig. 1a). A significant decrease in the magnitude of the spatial gradient in  $N_m$  is evident after 0200 AST. The variation of  $h_m$  with azimuth is somewhat harder to perceive (Fig. 1b). However, the persistent zonal gradient from 0100 to 0200 AST does stand out clearly.

Figure 2 shows the measured variation in  $h_m$ ,  $N_m$  and their horizontal gradients for two representative nights in December 1981. In Fig. 3, we show the same parameters for two nights in August 1982. Several features are illustrated by these two figures.

First, the average value of  $h_m$  is some 40 km higher

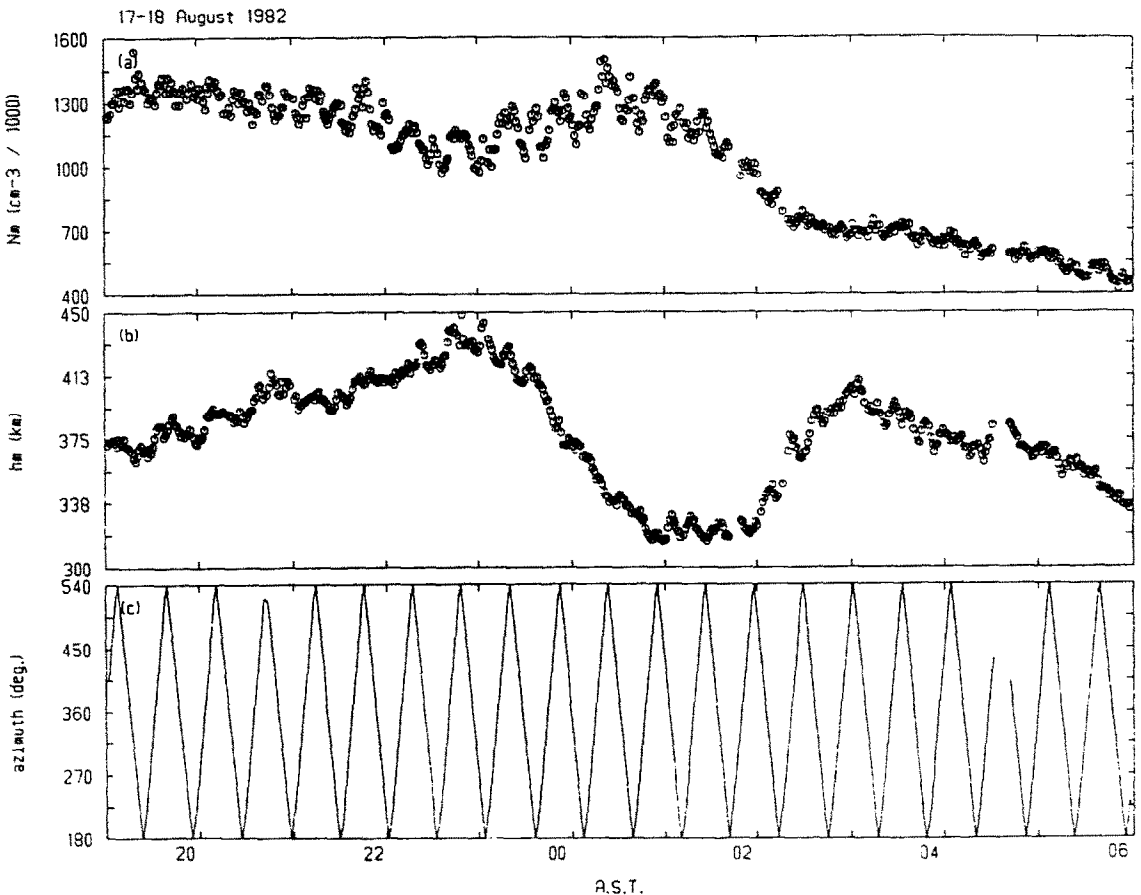


Fig. 1. The results obtained by fitting a Chapman function to individual electron density measurements on 17–18 August 1982. (a) Peak electron density; (b)  $h_m$ ; (c) the azimuth of the observation. The azimuth scan reverses direction at 180° (due south).

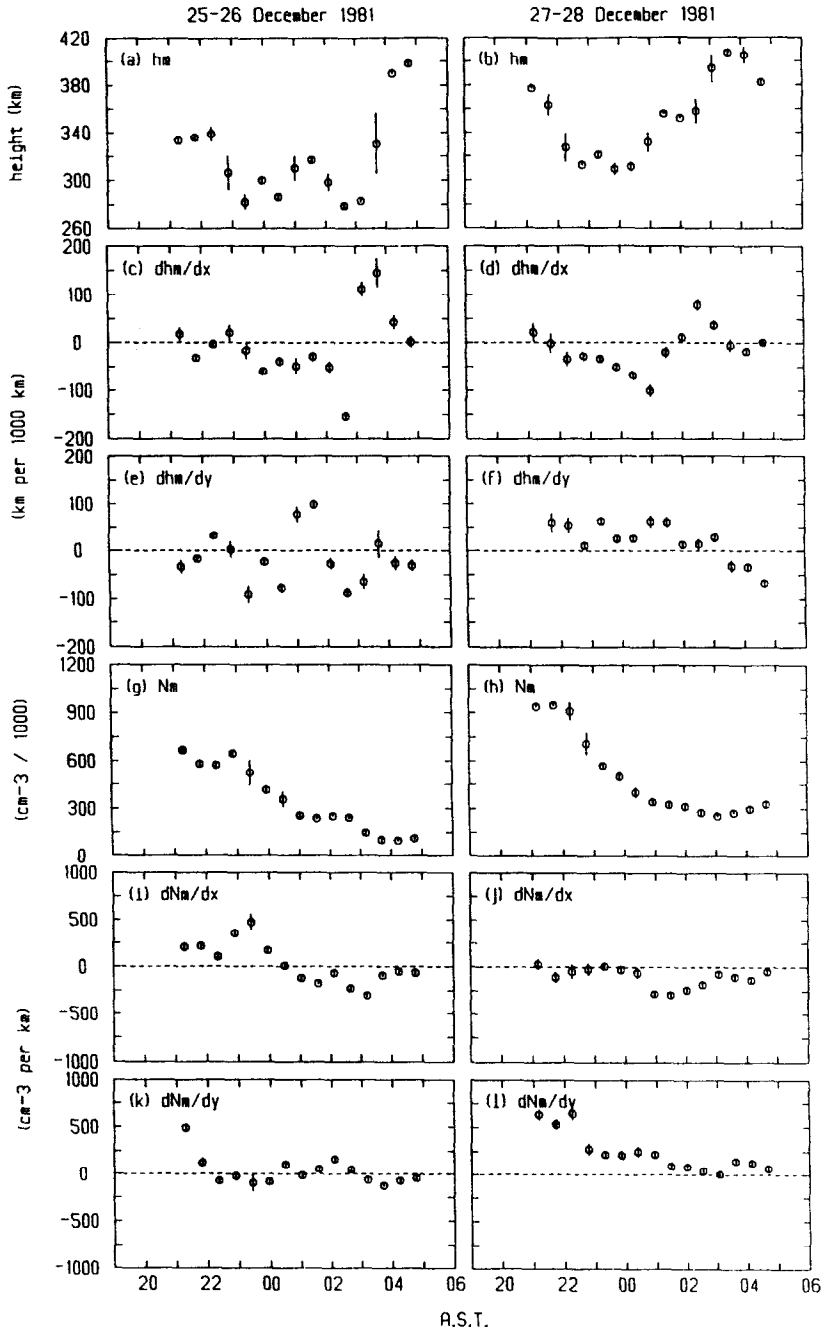


Fig. 2. A summary of the parameters of the *F*-layer peak at Arecibo on the nights of 25-26 December 1981 (left column) and 27-28 December 1981 (right column).

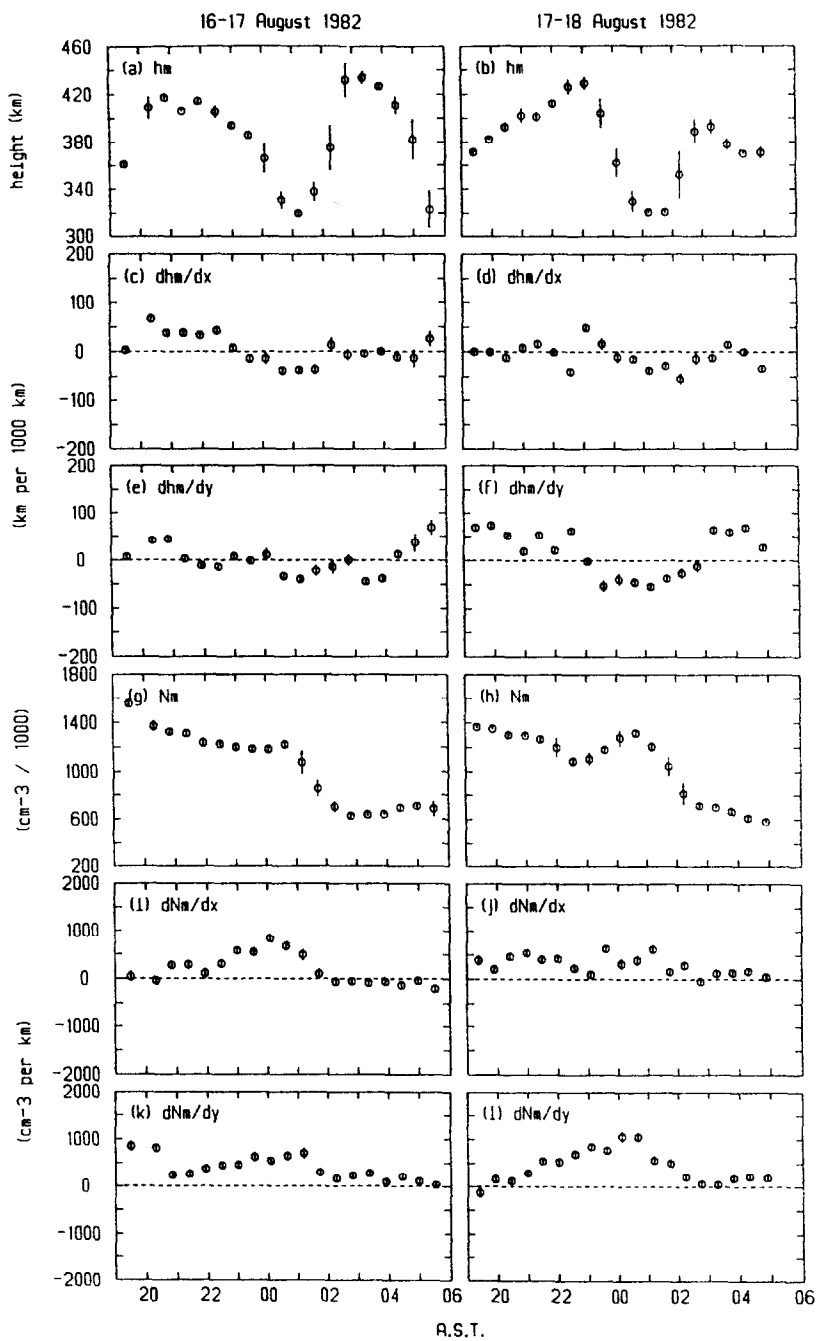


Fig. 3. The same parameters as shown in Fig. 2, but for two nights in August 1982. However, note that the scales for  $h_m$  (row 1) and  $N_m$  and its gradients (rows 4-6) are different from those in Fig. 2.

in August 1982 than it is in December 1981. At the same time,  $N_m$  is about twice as great in August 1982. This seasonal change in  $h_m$  has been reported previously by BURNSIDE *et al.* (1983b) and appears to be related to seasonal variations in the meridional component of the neutral wind velocity.

Second, a more or less well-defined 'midnight descent' of the  $F$ -layer occurs on each night. At the culmination of the  $F$ -layer descent,  $h_m$  is generally lower to the south of Arecibo than it is to the north. When  $h_m$  starts to rise again, the rise starts in the south. This effect is more evident in the December data (Fig. 2) than it is in August (Fig. 3).

Third, in August 1982 there is a persistent tendency for  $N_m$  to be largest to the southeast of Arecibo, at least until about 0300 AST, after which the horizontal gradients in  $N_m$  are often small. On most of the nights that we have analysed in December 1981 the gradient in  $N_m$  is small compared with the values in August 1982. However, the night of 27–28 December 1981 is unusual. The marked zonal gradient in  $N_m$  observed before midnight on this night [Fig. 2(1)] was not observed on the other December nights. It is possible that this difference is related to magnetic activity, as we discuss further in Sections 4 and 5.

#### 4. PLASMA TRANSPORT AT THE $F$ -LAYER PEAK

##### 4.1. The continuity equation

To see whether horizontal plasma advection is significant for the dynamics of the night-time  $F$ -layer at Arecibo, it is necessary to compare it with the other terms in the continuity equation. Assuming that the production of ionization may be neglected at night, the continuity equation may be written as

$$\frac{\partial N}{\partial t} = -\beta N - \mathbf{v} \cdot \nabla N - N \nabla \cdot \mathbf{v} \quad (1)$$

where  $N$  is plasma density,  $\mathbf{v}$  is plasma velocity and  $\beta$  is the loss rate. The last two terms on the right hand side of (1) give  $\nabla \cdot (N\mathbf{v})$ , which fully accounts for ion transport. Here, however, we treat these two terms separately, referring to  $\mathbf{v} \cdot \nabla N$  as the 'plasma advection term' and  $N \nabla \cdot \mathbf{v}$  as the 'divergence term'. In this work we assume that  $\beta$  is determined only by the charge exchange reactions of  $\text{O}^+$  with  $\text{O}_2$  and  $\text{N}_2$ , so that

$$\beta(z) = k_1[\text{O}_2](z) + k_2[\text{N}_2](z) \quad (2)$$

where  $k_1$  and  $k_2$  are the reaction rates for charge exchange with  $\text{O}_2$  and  $\text{N}_2$ , respectively. We use the temperature dependent expressions given by ST-

MAURICE and TORR (1978) to evaluate  $k_1$  and  $k_2$ . The most recent MSIS model (HEDIN, 1983) is used to supply the neutral densities.

The temporal derivative  $\partial N / \partial t$  and the horizontal components of  $\mathbf{v} \cdot \nabla N$  are determined directly from the incoherent scatter data. Also, we are only interested in evaluating (1) at the  $F$ -layer peak, where the contribution of vertical plasma advection is zero. However, the evaluation of  $\nabla \cdot \mathbf{v}$  is more difficult, because only one component of the velocity gradient ( $\partial v_z / \partial z$ ) is available from the measurements. In the Appendix, we show that the electrodynamic requirement that  $\nabla \times \mathbf{E} = 0$  leads to

$$\nabla \cdot \mathbf{v} = \frac{\partial v_z}{\partial z} + \cot I \frac{\partial v_z}{\partial x} \quad (3)$$

where  $v_z$  is vertical ion velocity,  $I$  is magnetic inclination ( $50^\circ$  at Arecibo) and  $x$  is positive southward. So, the only impediment to evaluating (1) with very few approximations is the lack of a direct measurement of  $\partial v_z / \partial x$ .

To estimate the horizontal variation of  $v_z$ , we have used an integrated form of the  $\text{O}^+$  continuity equation. Neglecting horizontal gradients in  $\mathbf{v}$ , integration of (1) gives

$$v_z(x, z) = -\frac{1}{N(x, z)} \int_0^z \left( \frac{\partial N(x, z')}{\partial t} + \beta(x, z') N(x, z') + v_x(z') \frac{\partial N}{\partial x}(z') + v_y(z') \frac{\partial N}{\partial y}(z') \right) dz' \quad (4)$$

so long as the lower boundary is low enough that the flux across it may be assumed to be zero. In practice we have evaluated (4) with  $z_0 = 180$  km and  $z = h_m$ , which is taken to be constant for the purposes of numerical evaluation. The overhead values of  $v_z$  derived using (4) may be checked by comparing them with direct radar measurements. In Fig. 4, the observed and calculated values of  $v_z$  are shown for two different nights. In general, the agreement between observation and calculation is good.

We can now obtain a first order estimate of the latitudinal gradient in  $v_z$  from

$$\frac{\partial v_z}{\partial x}(z) \simeq \frac{v_z(r, z) - v_z(0, z)}{r} \quad (5)$$

where  $r$  is the radius of the radar beamswinging circle at height  $z$ . We have no real choice but to assume that the last two terms in the integrand of (4) are independent of  $x$ . We cannot really determine whether or not this is a good assumption, but in any case it means that these terms have no influence on the derived values of  $\partial v_z / \partial x$ .

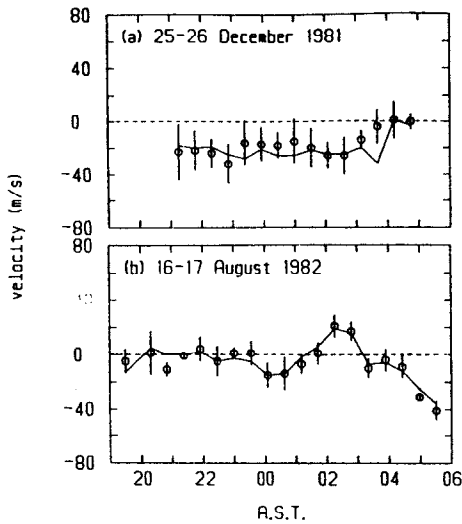


Fig. 4. The vertical ion velocities ( $v_z$ ) at the *F*-layer peak. (a) 25–26 December 1981; (b) 16–17 August 1982. Open circles show the values derived by integration of the continuity equation from 180 km up to the layer peak, using measured electron densities. The solid lines represent direct radar measurements of  $v_z$ .

#### 4.2. Results

By combining the derived gradients in  $N_m$  with the horizontal components of ion velocity at the same height, we have evaluated the equivalent rates of plasma production or loss due to horizontal advection for 19 nights between December 1981 and October 1983. Some results of these calculations are shown in Fig. 5. It is apparent that zonal advection is almost always more important than meridional advection. The loss of plasma due to zonal advection is usually most pronounced in the summer data that we have examined, and during the first half of the night. A similar effect is seen on only one of the four December nights that we have studied. The large values of zonal advection before midnight in August are maintained by the fairly substantial eastward ion velocities (typically  $50 \text{ m s}^{-1}$ ) at this time. By contrast, the meridional ion velocity tends to be smaller, thus reducing the importance of meridional advection, although north–south gradients in  $N_m$  are observed.

The values of  $\partial v_z / \partial x$  determined from (5) have been used in (3) to determine  $\nabla \cdot v$ . Figure 6 shows the derived values of  $\partial v_z / \partial z$  and  $\partial v_z / \partial x$ , as well as the resultant  $\nabla \cdot v$  for a winter and a summer night. We find that, in general, as on the two nights shown, the vertical gradient in  $v_z$  makes a somewhat larger

contribution to  $\nabla \cdot v$  than the horizontal gradient term in (3).

For each night we have calculated the plasma production or loss rates at the *F*-layer peak due to advection, divergence and chemical loss. In Figs. 7–11, we show detailed results for 5 specific nights in an attempt to illustrate the different types of behaviour that are observed at Arecibo. The zonal and meridional advection terms have been added to give the values of  $v \cdot \nabla N_m$  that are shown in panel (c) of these figures. By summing the advection, divergence and loss terms, we obtain the calculated values of  $\partial N_m / \partial t$  that are shown in panel (f). These results may be compared with the observed values of  $\partial N_m / \partial t$  that are shown as solid lines in panel (f) of Figs. 7–11. Although the calculated values of  $\partial N_m / \partial t$  show quite a lot of scatter, they often match the observed values fairly well. Frequently, the largest source of uncertainty is the divergence term. However, large uncertainties are sometimes present in the advection term as well, especially when the *F*-layer is high.

On the winter night shown in Fig. 7, the steady fall in  $N_m$  after 2200 AST is largely due to chemical loss, which becomes large as the *F*-layer descends to about 300 km. However, on 16–17 August 1982 (Fig. 8) chemical loss is very small between 2100 and 0000 AST and the gradual fall in  $N_m$  over this period is apparently due to horizontal (mainly zonal) advection. However, on another summer night, 17–18 June 1983, shown in Fig. 9, the balance of the continuity equation is quite different. Here, the increase in  $N_m$  observed before 2200 AST is due to convergent flow of the plasma. The role of convergent plasma flow in causing increases in  $N_m$  during the night at Arecibo was recognised by HARPER (1979). However, Harper did not attempt to assess its importance by direct comparison with the other terms in the continuity equation, as we do here.

The night of 4–5 October 1983 (Fig. 10) illustrates another type of behaviour. Here, horizontal advection is small, but loss and convergence tend to balance each other, with the result that  $N_m$  changes remarkably little over the whole night. The night of 4–5 October 1983 coincided with the recovery phase of a fairly substantial magnetic storm, unlike 9–10 October 1983 (Fig. 11), which was very quiet. On this night,  $N_m$  falls much more rapidly, with the exception of the period near 0200 AST when converging plasma flow causes a temporary increase in  $N_m$ .

Table 1 gives a synopsis of the results of our calculations using data obtained on 19 nights (from four observing campaigns) between December 1981

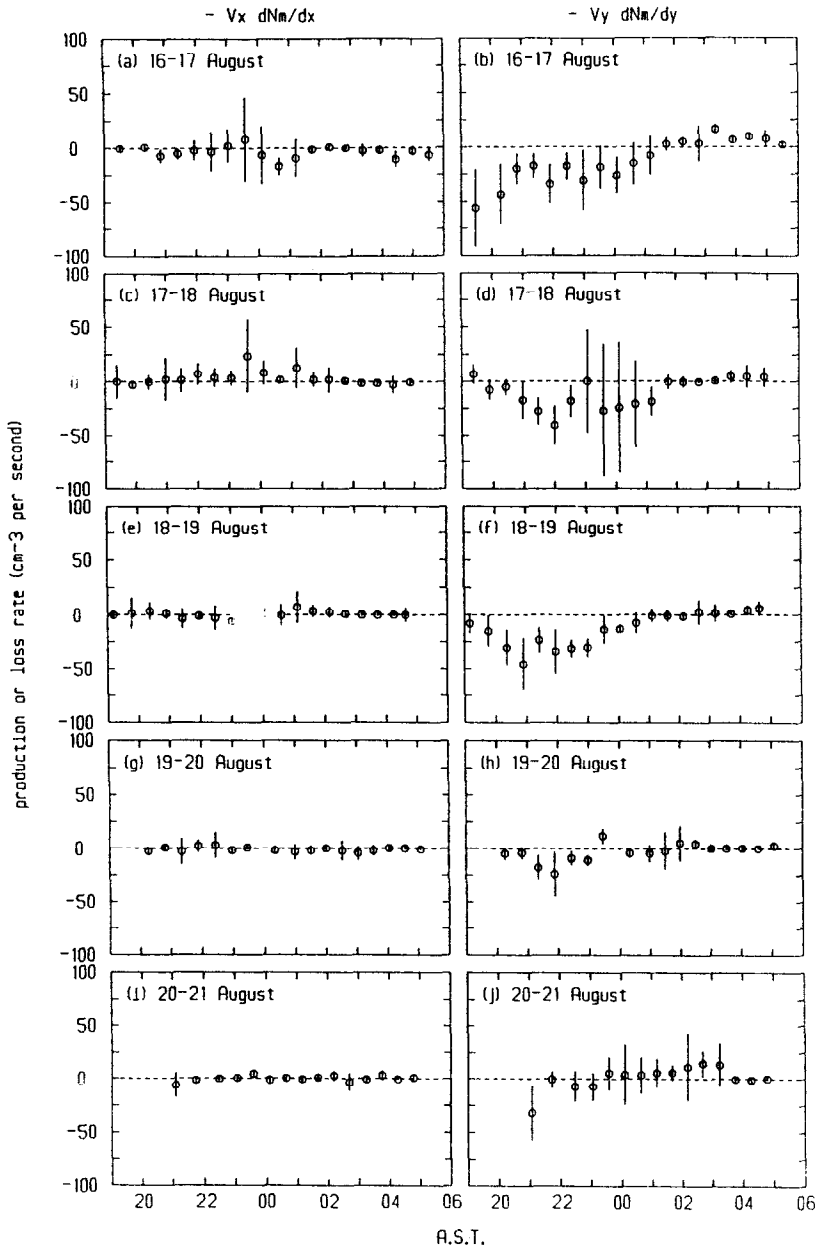


Fig. 5. The effective production or loss rate due to horizontal plasma advection at the *F*-layer peak for 5 nights in August 1982. The left column shows the meridional component of  $v \cdot \nabla N_m$  and the right column the zonal component.



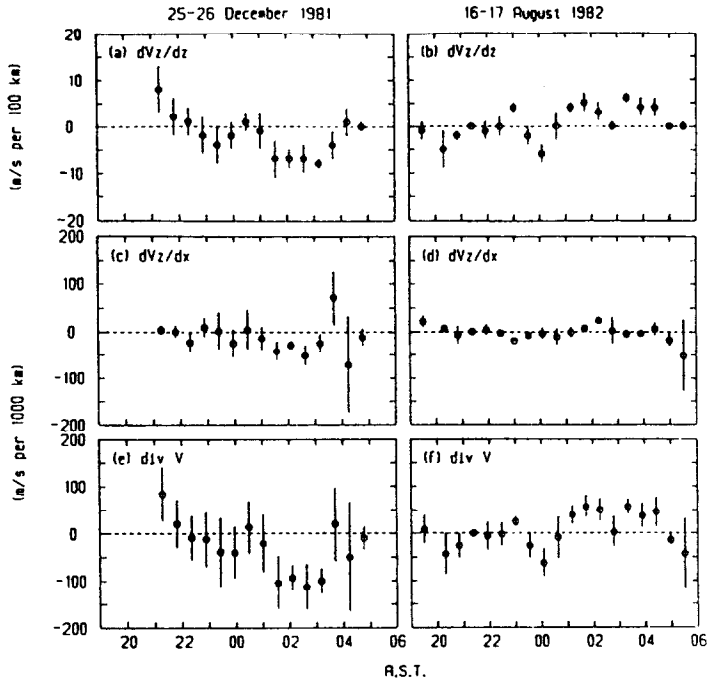


Fig. 6. The observed values of  $\partial v_z/\partial z$ . (a) 25–26 December 1981; (b) 16–17 August 1982. (c), (d) The inferred values of  $\partial v_z/\partial x$  for the same two nights. (e), (f) The resultant values of  $\nabla \cdot \mathbf{v}$  for these two nights.

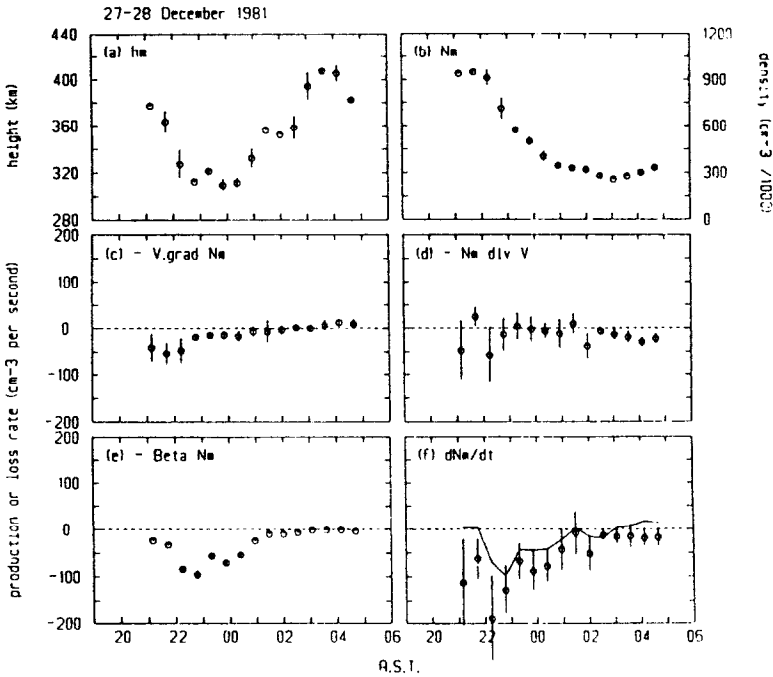


Fig. 7. Values of (a)  $h_m$ , (b)  $N_m$  and (c) the advection, (d) divergence and (e) loss terms in the continuity equation on 27–28 December 1981. In (f), the open circles represent the sum of (c), (d) and (e), while the solid line shows the value of  $\partial N_m/\partial t$  calculated from the observed values of  $N_m$ . Typical uncertainties in the direct estimate of  $\partial N_m/\partial t$  are about  $10 \text{ cm}^{-3} \text{ s}^{-1}$ .

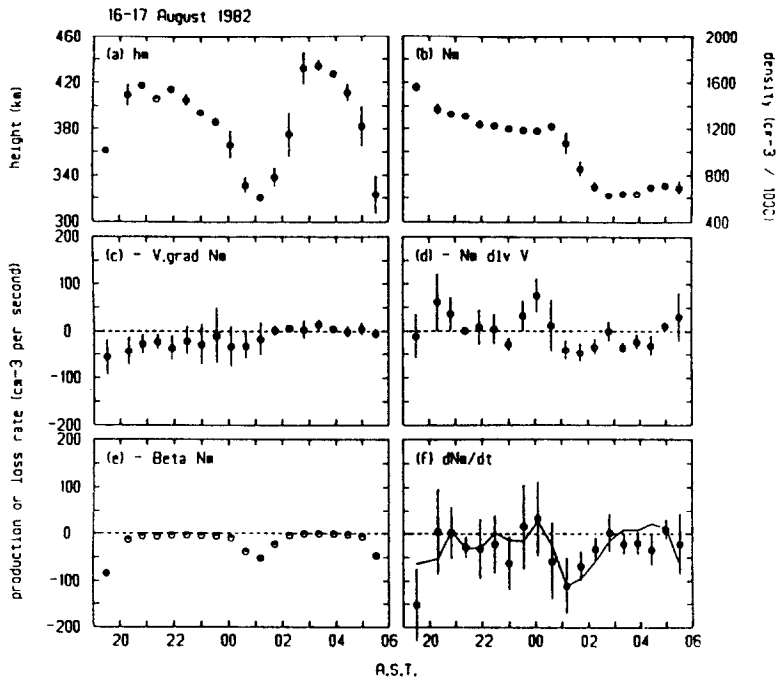


Fig. 8. As Fig. 7, but for 16-17 August 1982.

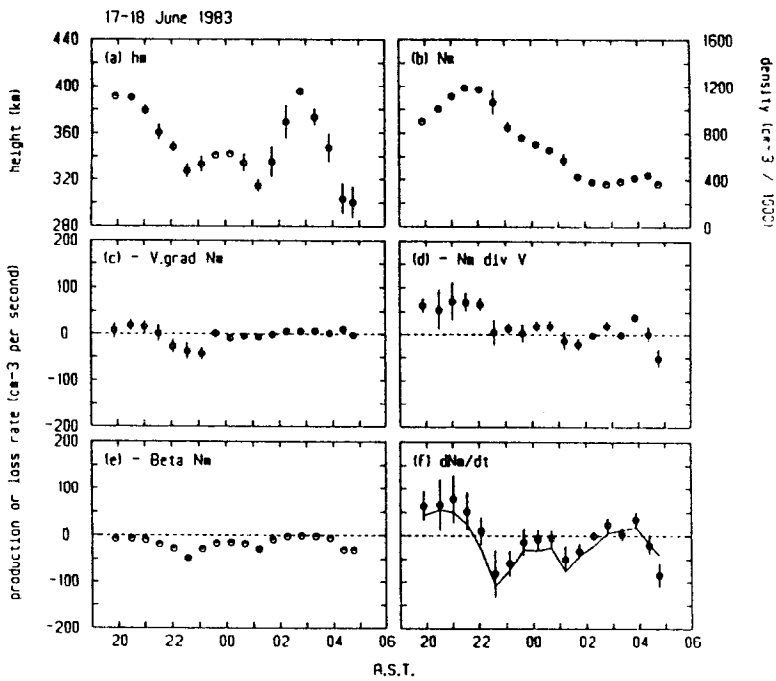


Fig. 9. As Fig. 7, but for 17-18 June 1983.

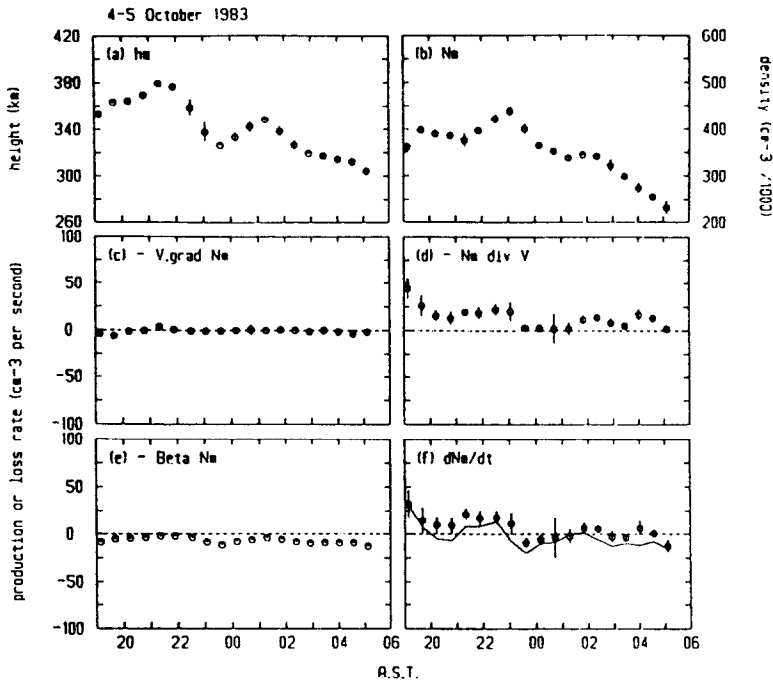


Fig. 10. As Fig. 7. but for 4-5 October 1983.

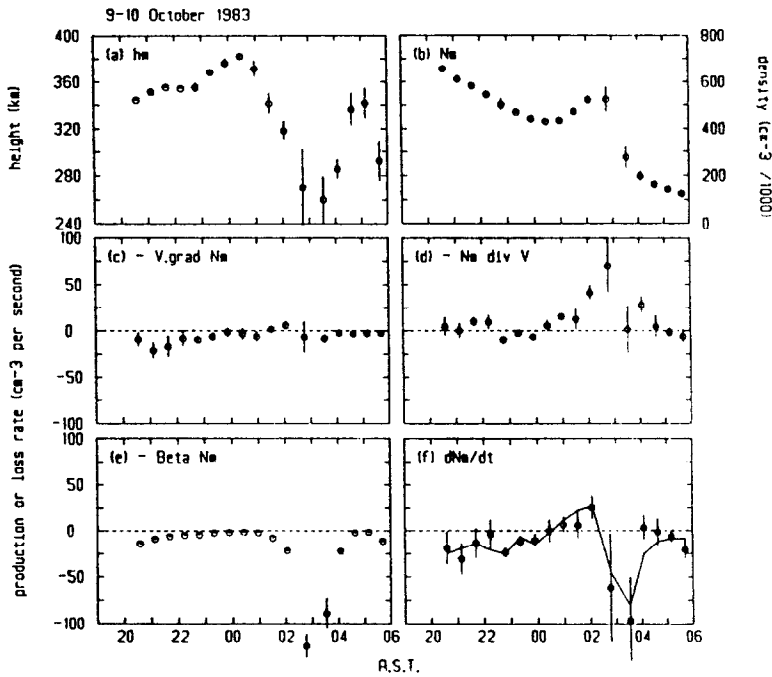


Fig. 11. As Fig. 7. but for 9-10 October 1983.

Table 1. Three hourly average values of  $h_m$  (km),  $N_m$  (units of  $10^6 \text{ cm}^{-3}$ ) and the effective production rates by the advection (A), divergence (D) and loss (L) terms in the  $\text{O}^+$  continuity equation

Starting date	Sa	Ap	2000-2300 AST						2300-0200 AST						0200-0500 AST								
			K	$h_m$	$N_m$	A	D	$N_t$	K	$h_m$	$N_m$	A	D	$N_t$	K	$h_m$	$N_m$	A	D	$N_t$			
23/12/81	156	10	4	320	0.6	0	-5	-6	3	360	0.4	0	-2	-1	-1	2	340	0.3	0	-1	0	0	
25/12/81	166	6	2	320	0.6	0	-1	-3	1	300	0.4	0	1	-5	-4	2	340	0.2	0	1	-1	-1	
26/12/81	177	6	1	320	0.6	0	-2	-6	0	320	0.4	0	-1	-3	-2	0	340	0.2	0	0	-2	-1	
27/12/81	183	12	2	340	0.8	-4	-2	-5	2	330	0.4	-1	0	-4	-2	2	380	0.3	0	-1	0	0	
16/8/82	165	16	1	410	1.3	-3	2	0	-2	4	360	1.1	-2	0	-3	-5	2	420	0.7	0	-2	0	0
17/8/82	166	16	3	410	1.2	-2	-1	-1	-2	3	360	1.2	-1	-2	-4	-4	2	380	0.7	0	0	0	-1
18/8/82	159	10	2	390	1.4	-4	1	-2	-2	2	350	1.2	-1	-2	-2	-2	1	350	0.8	0	-1	-1	-2
19/8/82	145	12	0	420	0.9	-1	0	0	-1	1	380	0.9	0	-2	-1	1	0	320	0.6	0	0	-3	-5
20/8/82	139	15	3	400	1.1	0	0	0	-1	3	390	1.0	0	1	0	0	1	340	0.8	0	0	-3	-5
13/6/83	126	12	3	380	1.1	0	4	-1	0	3	360	1.0	1	3	-3	-3	3	340	0.5	0	0	-1	-5
14/6/83	129	17	4	400	0.9	-2	3	0	0	4	370	0.9	0	2	-1	0	3	350	0.6	1	-1	-1	-4
15/6/83	129	8	1	370	1.1	-2	3	-1	-4	1	370	0.8	-1	2	0	-2	0	320	0.7	0	0	-2	-2
16/6/83	131	17	0	380	0.6	0	1	0	0	1	340	0.6	1	0	-2	-1	3	340	0.5	0	0	-1	-2
17/6/83	130	37	2	360	1.1	-1	5	-3	0	3	330	0.7	-1	0	-2	-5	4	350	0.4	0	0	-1	-1
4/10/83	127	8	1	370	0.4	0	2	0	0	2	340	0.4	0	1	-1	-1	2	320	0.3	0	1	-1	-1
5/10/83	133	22	2	370	0.3	-1	0	0	-1	2	320	0.3	0	2	-2	0	2	330	0.2	0	1	-3	-2
7/10/83	131	16	2	380	0.5	-1	0	0	-2	2	340	0.5	0	1	-2	0	1	320	0.2	0	0	-3	-2
8/10/83	130	5	2	330	0.6	-1	2	-3	-1	1	330	0.6	-1	2	-3	-1	1	320	0.3	0	1	-5	-3
9/10/83	134	7	0	350	0.6	-2	0	-1	-2	0	360	0.5	0	1	0	0	1	300	0.3	0	3	-6	-3
Mean 12/81	170	8		325	0.6	-1	-2	-5	-4	330	0.4	0	0	-3	-2		350	0.2	0	0	-1	-1	
Mean 8/82	155	14		405	1.2	-2	0	-1	-2	370	1.1	-1	-1	-2	-2		360	0.7	0	-1	-1	-3	
Mean 6/83	129	18		380	1.0	-1	3	-1	-1	350	0.8	0	1	-2	-2		340	0.5	0	0	-1	-3	
Mean 10/83	131	12		370	0.5	-1	0	0	-1	340	0.4	0	1	-2	0		320	0.3	0	1	-4	-2	

$N_t$  represents  $\partial N_m / \partial t$ , as calculated from the observed time rate of change of  $N_m$ . The production rates are given in units of  $10 \text{ cm}^{-3} \text{ s}^{-1}$ . Sa is the solar 10.7 cm flux. K indices are for San Juan, Puerto Rico.

and October 1983. Average values over 3 h time intervals are shown. This procedure might be questioned, especially as parameters like  $h_m$  and the various production rates often vary significantly in 3 h. However, we believe that the most important temporal and seasonal variations do become apparent in Table 1. Although there is really too little data in each season for good statistical analysis, the average values calculated for each month are also shown in Table 1.

### 5. DISCUSSION

Most of the data that we have examined exhibit horizontal gradients in both  $h_m$  and  $N_m$  that are significantly different from zero at some time of the night. The horizontal gradients in  $N_m$  tend to be larger in summer than in winter, but any seasonal variation in  $\nabla h_m$  is less obvious.

The large values of  $\partial N_m / \partial y$  shown in Fig. 3 might not have been expected. Any simple picture of the Earth rotating under an ionosphere fixed in local time turns out to be completely wrong. If that were the case, we would observe  $\partial N_m / \partial y$  to be proportional to  $\partial N_m / \partial t$ . In fact, however,  $\partial N_m / \partial y$  is almost always greater than zero, while  $\partial N_m / \partial t$  is usually small or negative [compare Figs. 3(k) and 8(f)]. In other words, at least so far as  $N_m$  is concerned, local time and longitude are by no means equivalent in the night-time *F*-layer at Arecibo. By examining Figs. 2 and 3, we also find that, while there are some periods when  $\partial h_m / \partial y$  is roughly proportional to  $\partial h_m / \partial t$ , there are many times when this is not so.

The tendency for the largest values of  $N_m$  to be observed to the east of Arecibo at night could partly be explained by the change in the declination of the magnetic field with longitude, which is fairly substantial near Arecibo (see, for example, DACHEV and WALKER, 1982). Some 250 km to the west of Arecibo, **B** is aligned about  $8^\circ$  west of geographic north (declination  $-8.0^\circ$ ), while 250 km to the east the declination is  $-10.7^\circ$ . Thus, a constant eastward neutral wind would have a larger component directed up along **B** to the east of Arecibo than to the west. This would tend to raise the *F*-layer east of Arecibo to a region of lower recombination, and thus allow higher electron densities to be maintained (see RISHBETH *et al.*, 1978). However, if this mechanism were operating alone, we would also expect  $N_m$  to be diminished to the east of Arecibo when the zonal wind (and ion flow) reverses, as it usually does at about 0200 AST in summer (BURNSIDE *et al.*, 1981).

In other words, we would expect  $\partial N_m / \partial y$  to change sign so that  $v_y \partial N_m / \partial y$  is always positive. However, this expectation is not really supported by the results shown in Figs. 3 and 5. For typical neutral velocities, the change of declination with longitude could lead to a difference of a few metres per second between the field-aligned wind component at locations 250 km east and west of Arecibo. It seems probable that spatial gradients in the neutral wind velocity (BURNSIDE *et al.*, 1981) could also produce effects of this order of magnitude.

It is well established (FUKAO *et al.*, 1979; EMERY *et al.*, 1981) that the night-time variation of  $N_m$  at Arecibo differs quite widely from one season to the next, and with magnetic activity. Because variations in  $N_m$  are controlled by three distinct terms in the continuity equation (1), a wide range of behaviour is clearly possible if different terms dominate (1) at different times. It may be seen from Figs. 7–11 and Table 1 that  $h_m$ ,  $N_m$  and the three terms that combine to give  $\partial N_m / \partial t$  do indeed vary quite significantly, both with season and from night to night. Comparison of the results on 4–5 and 9–10 October 1983 (Figs. 10 and 11) suggests that magnetic activity can certainly explain some of the night-to-night variability that is observed. However, our sample of disturbed nights is too small to allow any more definitive statement to be made.

In order to balance the  $O^+$  continuity equation for the night-time *F*-layer at Malvern, U.K., JAIN and WILLIAMS (1974) suggested that northward transport of plasma might be required. However, the situation at Arecibo appears to be quite different. Because the meridional ion velocity at Arecibo is generally small at night, zonal advection is actually more important than meridional advection, and it usually acts as a minor sink rather than a source of plasma. The results shown in Table 1 provide a strong indication that advection is largest before midnight, irrespective of season. This suggests that this effect is related to eastward plasma flow, rather than, for example, the height of the *F*-layer. In the period between 2000 and 2300 AST, the typical eastward ion velocity observed at Arecibo, both in December 1981 and August 1982, was about  $50 \text{ m s}^{-1}$  (BURNSIDE *et al.*, 1983a). The importance of horizontal advection is perhaps best illustrated by the results in the period from 2000 to 2300 AST in August 1982. In this month, plasma convergence is small throughout the night. Although zonal advection causes a local loss of plasma before midnight in August 1982, it never becomes large enough to cause a very rapid depletion in peak plasma density. Large loss rates are not observed

until  $h_m$  starts to fall, and these are well accounted for by recombination. On none of the nights that we have examined does horizontal advection provide a significant local source of plasma at the  $F$ -layer peak.

On those occasions that we observe increases in  $N_m$  at some time during the night, plasma convergence rather than horizontal advection is usually responsible. The role of converging plasma flow in opposing chemical recombination is especially apparent in the results from June 1983 (see Table 1). Between 2000 and 0200 AST in this month,  $N_m$  decays much more slowly than it would without plasma convergence. Also, in October 1983, after 2300 AST (when the  $F$ -layer is low) convergence of plasma appears to provide a source that to some extent counteracts chemical loss. In the winter at Arecibo, meridional neutral wind velocities are generally small (BURNSIDE *et al.*, 1983b) and there appears to be no effective transport mechanism that opposes the steady chemical loss of plasma at night. In fact, before midnight in December 1981, we find that the divergence term augments recombination at the  $F$ -layer peak, rather than opposes it.

A preliminary study of our data suggests that the divergence term in (1) is related to variations in the neutral wind in the field-aligned direction. Geomagnetic disturbances are also known to cause changes in the thermospheric neutral wind field (HERNANDEZ and ROBLE, 1984) and thus would be expected to affect the transport terms in the  $O^+$  continuity equation. The link between the neutral wind field and the balance of the continuity equation is a subject that requires further study.

In the Appendix we show that electrodynamic constraints provide us with a good method of evaluating  $\partial v_y/\partial y$  from measurements of the vertical gradient in  $v_{\perp}$ , since

$$\frac{\partial v_y}{\partial y} = -\sec I \frac{\partial v_{\perp}}{\partial z} \quad (6)$$

where  $I$  is the magnetic field inclination, as before. Initial calculations show that  $\partial v_y/\partial y$  is not necessarily negligible. By using electrodynamic relations such as (6), together with the  $O^+$  diffusion and continuity equations, it should be possible to deduce many of the nine spatial derivatives of  $v$  from incoherent scatter radar data. A closer examination of these spatial gradients would probably lead to a better understanding of the complex three dimensional patterns of plasma flow that characterise the ionosphere at Arecibo.

*Acknowledgments*—We thank the director and staff of the Arecibo Observatory for their support during this project. We particularly thank M. P. SULZER and C. A. GONZALES for their contributions to the ionospheric data-taking programs used at Arecibo. We have benefitted from valuable discussions with H. RISHBETH in the course of this work. This paper forms part of a Ph.D. dissertation by R. G. B., submitted to the University of Michigan, 1984. This work was supported by grants ATM 80-15316, ATM 81-16749 and ATM 84-03051 from the Atmospheric Research Section, National Science Foundation. The National Astronomy and Ionosphere Center is operated by Cornell University under contract with the National Science Foundation.

#### REFERENCES

- |  |       |  |
|--|-------|--|
| ANDERSON D. N.   | 1981  | <i>J. atmos. terr. Phys.</i> <b>43</b> , 753.        |
| BEHNKE R. A.   | 1979  | <i>J. geophys. Res.</i> <b>84</b> , 974.             |
| BEHNKE R. A. and HAGFORS T.  | 1974  | <i>Radio Sci.</i> <b>9</b> , 211.                    |
| BURNSIDE R. G., HERRERO F. A., MERIWETHER J. W. and WALKER J. C. G.                  | 1981  | <i>J. geophys. Res.</i> <b>86</b> , 5532.            |
| BURNSIDE R. G., WALKER J. C. G., BEHNKE R. A. and GONZALES C. A.                     | 1983a | <i>J. geophys. Res.</i> <b>88</b> , 6259.            |
| BURNSIDE R. G., BEHNKE R. A. and WALKER J. C. G.                                     | 1983b | <i>J. geophys. Res.</i> <b>88</b> , 3181.            |
| DOUGHERTY J. P.  | 1961  | <i>J. atmos. terr. Phys.</i> <b>20</b> , 167.        |
| EMERY B. A., HARPER R. M., GANGULY S., WALKER J. C. G. and GILES G. A.               | 1981  | National Astronomy and Ionosphere Center Report 163. |
| EVANS J. V.  | 1975  | <i>Planet. Space Sci.</i> <b>23</b> , 1611.          |
| EVANS J. V., HOLT J. M., OLIVER W. L. and WAND R. H.                                 | 1983  | <i>J. geophys. Res.</i> <b>88</b> , 7769.            |
| FUKAO S., SATO T., KIMURA I. and HARPER R. M.  | 1979  | <i>J. atmos. terr. Phys.</i> <b>41</b> , 1205.       |
| GONZALES C. A., KELLEY M. C., BEHNKE R. A., VICKREY J. F., WAND R. H. and HOLT J. M. | 1983  | <i>J. geophys. Res.</i> <b>88</b> , 9135.            |
| HAGFORS T. and BEHNKE R. A.  | 1974  | <i>Radio Sci.</i> <b>9</b> , 89.                     |
| HARPER R. M.   | 1973  | <i>J. atmos. terr. Phys.</i> <b>35</b> , 2023.       |

HEDIN A. E.	1983	<i>J. geophys. Res.</i> <b>88</b> , 10170.
HERNANDEZ G. and ROBLE R. G.	1984	<i>J. geophys. Res.</i> <b>89</b> , 9049.
HERRERO F. A. and MERIWETHER J. W.	1980	<i>J. geophys. Res.</i> <b>85</b> , 4191.
IMEL G., KLEVANS E. H. and CARPENTER L. A.	1981	<i>J. geophys. Res.</i> <b>86</b> , 9204.
JAIN A. R. and WILLIAMS P. J. S.	1974	<i>J. atmos. terr. Phys.</i> <b>36</b> , 417.
KELLY J. D.	1983	<i>Geophys. Res. Lett.</i> <b>10</b> , 1112.
RISHBETH H., GANGULY S. and WALKER J. C. G.	1978	<i>J. atmos. terr. Phys.</i> <b>40</b> , 767.
SCHUNK R. W. and WALKER J. C. G.	1970	<i>Planet. Space Sci.</i> <b>18</b> , 1319.
ST.-MAURICE J. -P. and TORR D. G.	1978	<i>J. geophys. Res.</i> <b>83</b> , 969.
VICKREY J. F. and KELLEY M. C.	1982	<i>J. geophys. Res.</i> <b>87</b> , 4461.
VONDRAK R. R. and RICH F. J.	1982	<i>J. geophys. Res.</i> <b>87</b> , 6173.

APPENDIX

In order to investigate bulk plasma motions in the *F*-region we neglect electric currents, so the plasma velocity, which is equal to both the ion and electron velocities, is given by

$$\mathbf{v} = \frac{1}{B^2} [\mathbf{E}_\perp \times \mathbf{B}] + v_\parallel \hat{\mathbf{s}} \tag{A1}$$

where  $\mathbf{E}_\perp$  is the perpendicular component of electric field,  $v_\parallel$  is the component of ion velocity in the direction of  $\mathbf{B}$  and  $\hat{\mathbf{s}}$  is the unit vector antiparallel to  $\mathbf{B}$ . Taking the divergence of (A1) gives

$$\begin{aligned} \nabla \cdot \mathbf{v} &= \frac{1}{B^2} [\mathbf{B} \cdot \nabla \times \mathbf{E}_\perp - \mathbf{E}_\perp \cdot \nabla \times \mathbf{B}] + \frac{\partial v_\parallel}{\partial s} \tag{A2} \\ &= \frac{\partial v_\parallel}{\partial s} \end{aligned}$$

as Maxwell's equation reduces to  $\nabla \times \mathbf{E} = 0$  for steady state conditions [DOUGHERTY, 1961] and  $\nabla \times \mathbf{B} = 0$  for a dipole field.

Three other relations follow from  $\nabla \times \mathbf{E} = 0$ . Making use of the fact that  $\mathbf{E} = -\mathbf{v} \times \mathbf{B}$ , and taking  $\mathbf{B}$  to be constant, we obtain

$$\frac{\partial v_y}{\partial y} = -\sec I \frac{\partial v_\perp}{\partial z} = \tan I \frac{\partial v_x}{\partial z} - \frac{\partial v_z}{\partial z} \tag{A3}$$

$$\frac{\partial v_x}{\partial z} = -\cot I \frac{\partial v_y}{\partial x} \tag{A4}$$

$$\frac{\partial v_x}{\partial y} = \operatorname{cosec} I \frac{\partial v_\perp}{\partial x} = -\frac{\partial v_x}{\partial x} + \cot I \frac{\partial v_z}{\partial x} \tag{A5}$$

where  $I$  is the magnetic inclination, and  $x$  is positive southward,  $y$  is positive eastward and  $z$  is positive upward. Using (A5), we have a second expression for  $\nabla \cdot \mathbf{v}$ , but one that involves spatial gradients of  $v_z$  only, i.e.

$$\begin{aligned} \nabla \cdot \mathbf{v} &= \frac{\partial v_x}{\partial x} + \frac{\partial v_y}{\partial y} + \frac{\partial v_z}{\partial z} \tag{A6} \\ &= \frac{\partial v_z}{\partial z} + \cot I \frac{\partial v_z}{\partial x} \end{aligned}$$

which is the same result that would be obtained by assuming horizontal stratification, but with a second term that may in principle be significant, especially at low geomagnetic latitudes.